

Molybdenum Oxide Cluster Ions in the Gas Phase: Structure and Reactivity with Small Molecules

Elena F. Fialko, Andrey V. Kikhtenko, Vladimir B. Goncharov,* and Kirill I. Zamaraev

Boreskov Institute of Catalysis, Pr. Akademika Lavrentieva 5, 630090 Novosibirsk, Russia

Received: May 14, 1997; In Final Form: August 27, 1997[⊗]

The combination of the Knudsen cell with a standard cubic ICR trapping cell produces a number of cluster ions of molybdenum oxides Mo_xO_y^+ ($x = 1-5$, $y = 1-15$). Ionization of molybdenum trioxide vapors by electron impact yields Mo_xO_y^+ with high oxygen-to-metal ratios. Collisions with vacuum gas lead to reduction of oxygen-saturated molybdenum oxide cluster ions and to fragmentation of Mo_xO_y^+ ions with $x > 3$, whereas dimers and trimers are relatively stable. Time and temperature dependencies of Mo_xO_y^+ concentrations suggested that $\text{Mo}_4\text{O}_{12}^+$ and $\text{Mo}_5\text{O}_{15}^+$ are the primary products of MoO_3 vaporization and other ions are the products of their fragmentation. A simple pair-potential model was used to calculate energy-optimized geometric structures of the clusters. The model identifies the most abundant clusters as having the lowest calculated energy per atom. The six-ring Mo_3O_9 cluster was found to be the most stable species, and molybdenum oxides with four and five metal atoms also include the six atom ring where one or two oxygen atoms are substituted for the MoO_3 group. Ion–molecular reactions of molybdenum oxide cluster ions with some small molecules have been studied. Mo_xO_y^+ ions readily oxidize the CO molecule to CO_2 . Reactions of Mo_xO_y^+ ions with cyclopropane occur through the activation of the C–C bond of cyclopropane. In general, different molybdenum oxides exhibit the same reactivity toward $\text{c-C}_3\text{H}_6$. Dimer and trimer ions undergo the ligand-exchange reactions with ammonia, and molybdenum oxide trimers Mo_3O_8^+ and Mo_3O_9^+ dehydrogenate the NH_3 molecule, yielding a complex with nitrogen.

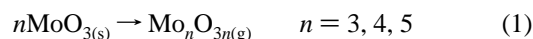
Introduction

The molybdenum-containing oxide catalysts are widely used in various fields of chemistry and oil refining.^{1–3} Studies of mechanisms of reactions proceeding over oxide catalysts are complicated by irregular structure of the active sites and adsorption, diffusion, and other processes. Gas-phase studies of the reactivity of molybdenum oxide ions with various neutral molecules using different types of mass spectrometric techniques allow to avoid these difficulties. Gas-phase reactions could be considered as the simplest model of interactions of the active sites of oxide catalysts with substrate molecules. Such studies can give an additional information concerning mechanisms of catalytic reactions.

Despite the importance of molybdenum oxides in the condensed phase, molybdenum oxide cluster ions have not been studied intensively by mass spectrometric methods mainly due to the presence of seven major molybdenum isotopes. This essentially complicates the spectra interpretation, especially in the case of cluster ions. There have been several studies of molybdenum oxide clusters using various mass spectrometric techniques and various methods of cluster ions generation.^{4–10} Most of the attention in earlier investigations has been focused on the production and fragmentation of cluster ions in the gas phase.

The sputtering of a pure molybdenum sample in the presence of oxygen in the secondary ion mass spectrometric experiments (SIMS) produced only monometallic molybdenum oxide ions (MoO^+ and MoO_2^+).⁴ Using the fast atom bombardment technique for sputtering of molybdenum di- and trioxide, primarily Mo_x^+ and Mo_xO_y^+ ions ($x = 1-3$, $y = 1, 2$) with low oxygen-to-metal ratios were yielded.⁵ The recombination reaction was found to be the dominant mechanism in Mo_xO_y^+ production.

The evaporation of oxide samples from the effusion source (Knudsen cell) is the other method of cluster oxide ion generation. The Knudsen effusion source together with the electron impact was also used to generate the molybdenum oxide clusters in the gas phase. For the first time Chupka and co-workers used mass spectrometry to determine the composition of vapor above MoO_3 directly.⁶ Vapor was shown to consist of molecules Mo_3O_9 , Mo_4O_{12} , and Mo_5O_{15} . Kazenas and Zvetkov^{7,8} studied molybdenum trioxide evaporation using platinum effusion chambers in the temperature range 800–1000 °C by high-temperature mass spectrometry. They proposed that molybdenum trioxide evaporates according to reaction 1:



A combination of thermal desorption with a triple quadrupole mass spectrometer was used for generation of molybdenum and tungsten oxide cluster anions $(\text{MoO}_3)_n^-$ ($n = 1-13$) and $(\text{WO}_3)_n^-$ ($n = 1-8$).⁹ The dissociative behavior of these ions and their reactions with oxygen- and sulfur-containing compounds were studied.

Laser vaporization is a convenient method to generate cluster ions. Michiel and Bijbels used laser microprobe mass analysis (LAMMA) in their study of cluster ion distribution of inorganic binary oxides.¹⁰ The authors showed that MoO_3 had a considerable contribution of MoO_2^+ ion intensity, and Mo_xO_y^+ oxide ions with $y > x$ were formed. However, they did not succeed in peak resolving for the high molybdenum oxide cluster ions.

Fourier transform ion cyclotron resonance (FT ICR) spectrometry is a convenient method to study gaseous ion–molecular reactions. Over the past decade gas-phase transition metal ion chemistry has been an active area of research.¹¹ For metal oxides, the reactions of FeO^+ ,¹² VO^+ ,¹³ and MoO_x^+ ($x = 1, 2$)¹⁴ with small hydrocarbons and the reactions of OsO_x^+ ($x = 1-4$)¹⁵ with some small molecules were investigated. These

[⊗] Abstract published in *Advance ACS Abstracts*, October 1, 1997.

investigations have indicated that reactivities of metal oxide ions depend on the number of vacant coordination places on a metal ion and on the M^+-O bond strength. There have been numerous studies of metal clusters and, more recently, metal oxide cluster ions using the FT ICR technique. For example, the reactivities of bare metal clusters including Nb_x^+ ,¹⁶ Fe_x^+ ,^{17,18} Co_x^+ , Rh_x^+ ,¹⁹ Cu_x^+ ,²⁰ and Ag_x^+ ²¹ with neutral substrates such as C_6H_6 , H_2 , NH_3 , C_2H_4 , $c-C_3H_6$, $c-C_6H_{12}$, and O_2 were examined, and ion–molecule reactions of $Ga_xO_y^+$, $In_xO_y^+$, $Al_xO_y^+$,²² $Al_xIn_yO_z^+$,²³ and $Co_xO_y^+$ ²⁴ clusters were investigated.

Direct laser vaporization (DLV) together with Fourier transform ion cyclotron resonance spectrometry (FT ICR) has been employed in investigations of production and fragmentation of molybdenum oxide ions.⁵ It was shown that DLV produced $Mo_xO_y^+$ ions with $x = 1-4$, $y = 0-12$ and relatively high oxygen-to-metal ratios. The coupling of the DLV technique and FT ICR made it possible to study the reactivity of produced ions. Cassidy and McElvany investigated the gas-phase reactions of produced Mo^+ , MoO^+ , and MoO_2^+ with small hydrocarbons.¹⁴

In this work the molybdenum oxide cluster ions generated with the Knudsen effusion source were studied using FT ICR spectrometry. It is found to be the most simple and inexpensive method of cluster ion generation. The $Mo_xO_y^+$ ($x = 1-5$, $y = 1-15$) cluster ions formed by electron impact are compared with $Mo_xO_y^+$ cluster ions produced by laser vaporization and fast atom bombardment reported by Cassidy and McElvany.⁵ Time and temperature dependencies of $Mo_xO_y^+$ cluster ion formation were studied to estimate ion behavior in reactions. Structures of molybdenum–oxygen clusters calculated using a simple pair-potential model are also discussed.

The reactions of $Mo_xO_y^+$ ions with CO , $c-C_3H_6$, and NH_3 were studied. To probe the reactivity of $Mo_xO_y^+$ ions, certain neutral reagents were chosen for two reasons. First, the conversions of these reagents are catalyzed by the solid molybdenum trioxide. That is why it was interesting to study the elementary steps of these reactions using the FT ICR method. Second, different reactivities of molybdenum oxide ions with the different number of molybdenum atoms can be achieved.

Experimental Section

All experiments were carried out on a standard Bruker-Spectrospin ion cyclotron resonance spectrometer CMS-47 described elsewhere.²⁵ This apparatus was equipped with a 33 mm cubic trapping cell and an Oxford Instruments vertical type superconducting magnet maintained at 4.7 T. The room-temperature bore of the magnet was 89 mm. The vacuum system was evacuated by means of an ionic pump with a capacity of 160 L/s. Background pressure was about 3×10^{-9} mbar. The Bayard-Alpert ionization gauge was used to monitor the pressure. Pressures of the reagents were $(2-7) \times 10^{-7}$ mbar. All reagents were commercially available (“Reachim”). The MoO_3 sample containing 97% isotope ^{98}Mo (v/o “Izotop”) was used to simplify the FT ICR spectra analysis. Gaseous reagents were used without additional purification. Standard pulsed frequency excitation and image current detection techniques were used. Several dozen spectra were signal averaged to enhance the signal-to-noise ratio. An accuracy of measurements of the ionic products was about 10%.

In ambiguous cases, reaction sequences were confirmed with the standard double-resonance technique, in which suppression of the daughter ion is sought by ejection of the supposed parent.²⁶ Moreover, some ions were excited with the cyclotron frequency (kinetic activation) in order to increase their energy that results in ion dissociation.

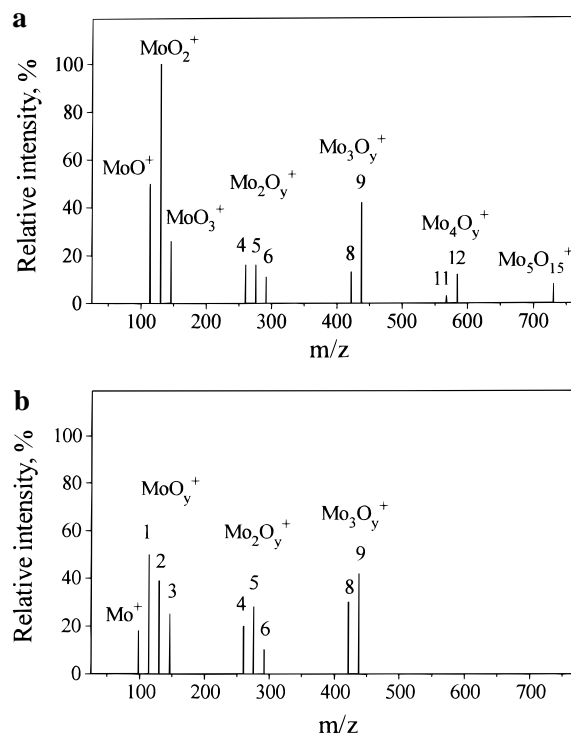



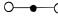
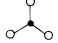
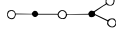
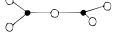
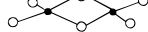
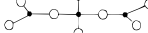
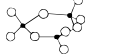
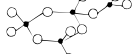
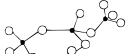
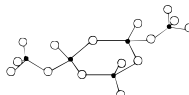
Figure 1. Positive ion spectrum of molybdenum trioxide ($^{98}MoO_3$) produced using the combination of Knudsen cell with ICR spectrometer at 650 K (a) and the same spectrum recorded after addition of CO , $P(CO) = 1.8 \times 10^{-7}$ mbar (b).

Molybdenum oxide cations were produced by 70 eV electron impact of molybdenum trioxide vapors. To evaporate molybdenum trioxide, the standard ICR trapping cell was modified with the self-made quartz Knudsen cell placed directly on the lower plate of the ICR cell. The ratio of the inner surface area of the crucible to the effusion hole area was approximately 1500 which provided effusion evaporation. The Knudsen cell was equipped with a bifilar heater. The temperature of the Knudsen cell was calibrated beforehand using a chromel–alumel thermocouple and Al_2O_3 powder as a standard sample. During the experiments the temperature in the Knudsen cell varied from 450 to 900 K in accordance with the current on the heater.

Results and Discussion

Formation of Cluster Ions. The combination of the Knudsen cell with an ICR trapping cell produces cluster ions $Mo_xO_y^+$ with the different number of molybdenum and oxygen atoms: $x = 1-5$, $y = 1-15$. A mass spectrum obtained by the vaporization of $^{98}MoO_3$ from the Knudsen cell at 700 K is shown in Figure 1a. MoO^+ , MoO_2^+ , and $Mo_3O_9^+$ are the most abundant products in our study, while Mo^+ is not observed. Intensities of molybdenum oxide ions decrease with the increase of molecular mass. Cluster ion production is affected by the energy of an electron impact, with the intensities of larger $Mo_xO_y^+$ decreasing as the energy increases. Kazenas and co-workers have observed similar phenomena.⁷ They have shown that $Mo_3O_9^+$, $Mo_4O_{12}^+$, and $Mo_5O_{15}^+$ were the primary products at 8 eV. While monomers and dimers appeared at 16 eV, they were the products of large cluster fragmentation during an electron impact. However, large clusters can dissociate not only during the electron impact but also during the collisions with vacuum gas (CO , CO_2 , H_2O). Studies of $Mo_xO_y^+$ ($x = 3, 4$) fragmentation using low-energy kinetic activation (1–3 eV) result in elimination of MoO_3 fragments (good agreement with previous data^{5,9}) and also abstraction of an oxygen atom. Activations with higher energy (> 5 eV) involve additional loss

TABLE 1: Bond Energies with Oxygen and MoO₃ in Positive Charged Molybdenum Oxides (kcal/mol), Calculated Low-Energy Structures of Molybdenum Oxide Clusters, and Energies per Atom in These Clusters (kcal/mol)

	calcd M ⁺ -O bond energy	calcd M ⁺ -MoO ₃ bond energy	exptl M ⁺ -O bond energies	calcd low-energy structure	energy per atom
MoO	98.5		<151 ^a		-80.1
MoO ₂	121		<127, ^b >118, <151 ^a		-92.5
MoO ₃	83		<127, ^b >85, <118 ^a		-89.7
Mo ₂ O ₄					-85.8
Mo ₂ O ₅					-90.8
Mo ₂ O ₆	56	111.5	<127 ^b		-89.0
Mo ₃ O ₈					-88.7
Mo ₃ O ₉	58	86	<127 ^b		-94.5
Mo ₄ O ₁₁					-82.6
Mo ₄ O ₁₂		73			-85.6
Mo ₅ O ₁₅		78			-83.6

^a Kikhtenko, A. V.; Goncharov, V. B.; Zamaraev, K. I. *Catal. Lett.* **1993**, *21*, 353. ^b This work.

of MoO₃ units and formation of greater amounts of oxygen-deficient oxide ions.

Cassady et al. have shown that FAB led to the formation of Mo_x⁺ and Mo₂O_y⁺ with fewer oxygens than the original sample stoichiometry suggested. DLV gave more highly oxygenated ions.⁵ However, ions with stoichiometry MoO₃ were not observed in DLV spectra. The vaporization from the Knudsen cell followed by an electron impact produces great amounts of molybdenum oxide cluster ions with a high oxygen-to-metal ratio. This method of cluster ion generation allows to obtain molybdenum oxide cluster ions more oxygenated than other methods do. The stoichiometry of produced Mo_xO_y⁺ ions is close to that of bulk MoO₃. This makes it interesting to study the reactivity of molybdenum oxides with different oxygen-to-molybdenum ratios and to compare it with the properties of a solid MoO₃ catalyst. Such an investigation can help to answer the question of what role molybdenum-oxygen units play as active sites of molybdenum oxide catalyst in different reactions.

Temperature Dependence. Temperature dependencies of Mo_xO_y⁺ concentrations were studied in the temperature range 450–750 K. MoO₃ vaporization begins at the temperature of about 470 K. At this temperature Mo₅O₁₅⁺ and Mo₄O₁₂⁺ ions and some amounts of Mo₃O₉⁺ ions were present in the gas phase. This fact suggests that MoO₃ vaporization occurs through reaction 1. As temperature increases, the total pressure in the system increases, too. A heated Knudsen cell is known to produce CO in significant amounts.²⁷ In our experiments CO⁺ was observed directly in mass spectra. The formation of CO is consistent with the decrease in Mo_xO_y⁺ production. In addition, the CO molecule can react with molybdenum oxide ions in two ways. First, these reactions may enhance the formation of oxygen-deficient cluster ions. Second, fragmentation of large oxides could occur, yielding more stable monomers, dimers, and trimers. The formation of dimers and trimers begins

at 550 K. Further heating to 650 K leads to the appearance of Mo⁺ in the gas phase.

The temperature dependencies allow to obtain individual heats of sublimation. This values for the dominant gaseous species were obtained by utilizing the Clausius–Clapeyron equation. The positive ion intensity associated with a partial pressure is related to the ion intensity by eq 2.²⁸ Hence, a semilog plot of I⁺T versus 1/T yields -ΔH as the slope.

$$p = kI^+T \quad (2)$$

In this way, the values of sublimation heats of Mo₃O₉, Mo₄O₁₂, and Mo₅O₁₅ were obtained. They are 64.7 ± 5.5, 70.6 ± 3.9, and 102.6 ± 6.1 kcal/mol, respectively. These values are somewhat lower than the data of ref 6, where sublimation heats were determined over the temperature range 840–880 K. As far as in our conditions Mo_xO_y destruction begins at a temperature of about 550 K; sublimation heats were calculated in temperature range 470–550 K. This may cause the differences in the values.

Bond Energies in Mo_xO_y⁺. Bond energies in the molybdenum oxide cluster ions estimated using thermochemical cycle (3) are presented in Table 1. Values for bond energies in neutral molybdenum oxides D°(M–O) and ionization potentials (IP) were taken from ref 29. For bond energies in Mo_xO_y⁺ with x > 3 we use data for neutral oxides, assuming insignificant difference of ionization potentials.

$$D^\circ(\text{M}^+-\text{O}) = D^\circ(\text{M}-\text{O}) + \text{IP}(\text{M}) - \text{IP}(\text{MO}) \quad (3)$$

According to the data of Table 1, molybdenum oxide ions with the stoichiometry MoO₃ have the weakest bond energies with oxygen, whereas dimers and trimers have a special fragmentation stability; i.e., their fragmentation should occur

TABLE 2: Product Ion Distribution for the Reactions of Mo_xO_y^+ Ions with $c\text{-C}_3\text{H}_6$

	MoO^+	MoO_2^+	MoO_3^+	Mo_2O_4^+	Mo_2O_5^+	Mo_2O_6^+	Mo_3O_8^+	Mo_3O_9^+
$\text{Mo}_x\text{O}_y(\text{C}_3\text{H}_4)^+$	100							
$\text{Mo}_x\text{O}_{y-1}(\text{C}_3\text{H}_4)^+$		15	100	36	34	100	32	100
$\text{Mo}_x\text{O}_y(\text{CH}_2)^+$		20		64	34		15	
$\text{Mo}_x\text{O}_y(\text{C}_2\text{H}_4)^+$		23			16			
$\text{Mo}_x\text{O}_y(\text{CH}_4)^+$		42			16		53	

rather slow. Thus, reactions occurring with the oxygen transfer are more likely than reactions of Mo_xO_y^+ fragmentation.

Mo_xO_y Structures. We investigated structures of the molybdenum oxide cluster ions using a simple pair-potential model. The geometries were obtained by minimizing the total potential energy of the cluster. The energy was calculated as a pairwise sum of Coulombic interactions and Born–Mayer repulsion.³⁰ The geometries were optimized with the use of the potential function

$$U_i = U_{\text{MO}} + U_{\text{MM}} + U_{\text{OO}} \quad (4)$$

$$U_{ij} = \frac{q_i q_j}{r_{ij}} + A \exp\left[-\frac{r_{ij}}{\rho}\right] \quad (5)$$

where r_{ij} is the internuclear distance between each pair of atoms, q_M and q_O are the atomic charges determined by stoichiometries of the observed cluster ions, and A and ρ are adjustable parameters obtained by requiring them to give the nearest-neighbor distance for the monomer and for the bulk solid. The values used for the calculations were $A = 2256 \text{ e}^2/\text{\AA}$, and $\rho = 0.181 \text{ \AA}$. For the molybdenum oxide clusters values of $q_M = +3$ and $q_O = -1$ were used to describe the clusters, given the observed stoichiometries from the experiment. The pair-potential model cannot account for metal–metal bonding. However, there is no evidence in collision spectra of any fragments where there could be a Mo–Mo bond. The same model was used to calculate structures of cobalt–oxygen^{31,32} and titanium–oxygen³³ cluster ions. Freas and Campana had shown that stoichiometrically equivalent and deficient (metal or oxygen) clusters had structural differences.

Several low-energy isomers are found by the model for each cluster. Optimal structures determined for the molybdenum oxide clusters are shown in Table 1. Energies per atom of the lowest energy isomers are also presented in the table. The most abundant cluster ions in the mass spectrum (Figure 1a) have the lowest energy per atom since ions with the lowest energy per atom should be energetically more stable. Homologues of each classes retain some structural similarities. In particular, the lowest energy isomers of the oxygen-deficient clusters are seen to be linear with less amount of bridging oxygen atoms. On the other hand, the stoichiometrically equivalent clusters have more thermal and bridge oxygen atoms, especially for lowest energy isomers.

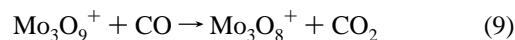
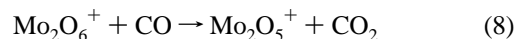
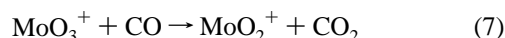
There are two groups of clusters: linear and ring. For linear clusters $\text{Mo}_x\text{O}_{3x-2}$ cluster structures are found to be the most unstable (MoO^+ and Mo_2O_4^+). Yet, they are observed in significant abundance in mass spectra. Probably, these cluster ions arise from rapid fragmentation of larger cluster ions. Linear molybdenum oxides with general stoichiometry $\text{Mo}_x\text{O}_{3x-1}$ are the most stable, and they are found to consist of the most abundant clusters in mass spectra. Mo_xO_{3x} clusters are less abundant. This may be due to the following two reasons. First, these clusters have higher energy per atom. Second, the thermal oxygen atoms can be removed by collision activation and reactions.

Six-ring Mo_3O_9 cluster has the lowest energy per atom, and it should be the most stable species. As bond energies indicate,

Mo_3O_9^+ can easily lose a thermal oxygen atom; however, it requires more energy to pull out a bridge oxygen atom (data in Table 1). It should be expected that the reactivity of Mo_3O_9^+ cluster ion will be different from reactions of monomers and dimers due to structural differences of the compounds. It seems that chemical properties of compact ring group of atoms should be closer to that of solid MoO_3 . Moreover, the presence of positive charge on such a big molecule has an insignificant effect due to the charge distribution.

As our calculations indicate, the lower energy structures for molybdenum oxides with four and five metal atoms also include the six-atom ring where one or two oxygen atoms are substituted for a MoO_3 group. Thus, these cluster ions can readily fragment yielding both Mo_3O_9^+ and MoO_3^+ ions. As was mentioned above, we did not study the reactivity of large oxide ions. However, probably, their reactions should occur through the loss of one or two MoO_3 fragments and formation of Mo_3O_9^+ –(substrate) intermediates.

Reactivity of Mo_xO_y^+ Ions. Reactions with CO. The addition of CO to the reaction medium was accompanied by the formation of the greater amounts of oxygen-deficient oxide ions, such as Mo^+ , MoO^+ , MoO_2^+ , Mo_2O_5^+ , and Mo_3O_8^+ (Figure 1b). This is due to the additional collisions and gas-phase reactions of CO oxidation, reactions 6–9.



CO_2 elimination indicates that $D^\circ(\text{MoO}^+-\text{O})$, $D^\circ(\text{MoO}_2^+-\text{O})$, $D^\circ(\text{Mo}_2\text{O}_5^+-\text{O})$, and $D^\circ(\text{Mo}_3\text{O}_8^+-\text{O})$ are less than 127 kcal/mol. These data well agree with the data of Table 1. In other attempts to bracket the strength of these bonds O atom transfer was sought from N_2O ($\text{Mo}_x\text{O}_{y+1}^+ + \text{N}_2$) and O_2 ($\text{Mo}_x\text{O}_{y+1}^+ + \text{O}$). There were reactions, undoubtedly, in all cases, but they resulted in a fast destruction of molybdenum oxide ions.

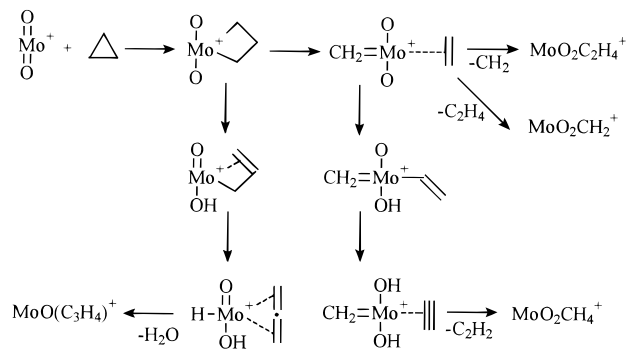
Reactions with $c\text{-C}_3\text{H}_6$. Shilling and Beauchamp had shown that in reaction with cyclopropane Mo^+ yielded dehydrogenation products.³⁴ Mo^+ was found to insert into the C–C bond rather than in the C–H bond, as far as the C–H bond strength of cyclopropane is 106 kcal/mol, while the C–C bond is much weaker, being only 54 kcal/mol.

The addition of oxygen atom to Mo^+ does not changes the reactivity of the metal species. Table 2 contains product ion distribution for the reactions of Mo_xO_y^+ ($x = 1-3$, $y = 1-9$) with cyclopropane. The extensive dehydrogenation that occurs in Mo^+ reactions is also observed for MoO^+ , reaction 10.



Here the oxygen atom is not involved in the reaction. Freiser and Beauchamp et al. had shown that participation of oxygen in reactions depends mostly on the M^+-O bond energy.

SCHEME 1



Thus, the reactivity of FeO^+ ($D^\circ = 81.4$ kcal/mol),¹³ CrO^+ ($D^\circ = 85.3$ kcal/mol),³⁵ and OsO^+ ($D^\circ = 100$ kcal/mol)¹⁵ increases in contrast to that of “bare” metal ions. This phenomenon is explained by the new exothermic reaction pathways producing such stable ligands as OH and H_2O . However, VO^+ reactivity is somewhat lower than that of V^+ ,¹³ since the bond energy of V^+-O is rather high ($D^0 = 133$ kcal/mol), so the oxo ligand is not involved in the oxidative reactions. The Mo^+-O bond is strong with a bond energy > 114 kcal/mol,³⁶ and it should not cleave in this reaction.

In their work Cassady and McElvany¹⁴ have shown that oxo ligand is only a spectator in the gas-phase reactions of MoO^+ with hydrocarbons. This suggestion is confirmed by the fact that the oxo ligand in MoO^+ does not actively participate in reaction with cyclopropane. Thus, a proposed mechanism of MoO^+ reaction with cyclopropane includes initial Mo^+ insertion into the C–C bond to form a metallacycle. Two β -H transfers and H_2 elimination yield a MoO^+ -allene complex. This mechanism is the same as that discussed for Mo^+ .³⁴

Mo^+ insertion into the C–H bond of cyclopropane can lead to the same product. However, as it was mentioned above, the C–H bond is very strong, and we proposed that its cleavage does not play a significant role in the formation of product ion.

Reactions of MoO_2^+ with cyclopropane dramatically differ from the MoO^+ reactions. The data in Table 2 indicate that MoO_2^+ readily loses one oxo ligand to produce $\text{MoOC}_3\text{H}_4^+$ and water molecule, reaction 11. This suggests that as the number of ligands bound to Mo^+ increases, the attachment of O and H atoms on the metal center to produce H_2O becomes more favorable.



However, MoO_2^+ dehydrogenates cyclopropane to a lesser extent than MoO^+ . The major reaction pathway is an extensive C–C bond cleavage accompanied by formation of $\text{MoO}_2\text{CH}_2^+$, $\text{MoO}_2\text{C}_2\text{H}_4^+$, and $\text{MoO}_2\text{CH}_4^+$ ions, reactions 12–14.



A proposed mechanism for the formation of the products for the reactions with cyclopropane is presented in Scheme 1. Initially, the molybdenum dioxide ion inserts into a C–C bond to form the molybdenum–cyclobutane ion **I**. Cleavage across the metallacycle yields intermediate **II**, which can lose ethene, reaction 13, or CH_2 , reaction 12. However, conversion of **I** to **II** is a $[2 + 2]$ reaction, originally forbidden by Woodward–

Hoffmann orbital symmetry rules. Theoretical considerations maintain that this concerted reaction becomes orbitally allowed when the bonding involves metal orbitals having primary d-character.³⁷ The differences in reactivity between Mo^+ , MoO^+ , and MoO_2^+ can be explained by noting that Mo^+ and MoO^+ ions have substantially more s-character to their bonding than MoO_2^+ .

A natural mechanism of $\text{MoO}_2\text{CH}_4^+$ formation, reaction 14, is subsequent dehydrogenation of intermediate **II**; C_2H_2 must be a neutral product for this process.

A mechanism of cyclopropane dehydration is also shown in Scheme 1. This mechanism is equal to the mechanism of the Mo^+ and MoO^+ reactions. However, the decreased number of sites available on molybdenum facilitates transfer of a H atom to an oxygen atom rather than bonding to the metal. But it is not clear whether the O–H coupling occurs during the first H transfer or the second one.

Mo^+ is a d^5 -system allowing only five covalent bonds to the metal ion in the gas-phase reactions. In solution oxomolybdenum groups are generally considered to involve double bonds. However, to explain the formation of some products, some steps in MoO_2^+ reactions must involve molybdenum-to-oxygen bonds with single-bond character. The nature of the Mo^+-O bonding at each step in Scheme 1 is unknown.

MoO_3^+ reactions with cyclopropane are limited to dehydration. MoO_3^+ is slightly faster to react than MoO_2^+ . As far as Mo^+ has only five electrons, one oxygen ligand must have a single bond with the metal ion. Thus, MoO_3^+ is a radical with a vacant electron on oxygen atom that makes it more reactive. MoO_3^+ abstracts a hydrogen atom from c- C_3H_6 . Since coordinative saturation is achieved, insertion of Mo^+ into cyclopropane bonds is impossible. The reaction should occur through Mo^+-O insertion into the C–C bond of cyclopropane. Since Mo^+ has no vacant places, the formation of carben products is not observed.

The four major reaction pathways of Mo_xO_y^+ are demonstrated in MoO_y^+ reactions: dehydration and elimination of CH_2 , C_2H_4 , and C_2H_2 are also observed in Mo_2O_y^+ and Mo_3O_y^+ ion reactions (see Table 2). The increase of the size of molybdenum oxide clusters does not affect the reactivity in the case of cyclopropane.

Loss of C_2H_4 is a major process in the reaction with Mo_2O_4^+ . The formation of $\text{Mo}_2\text{O}_4\text{C}_2\text{H}_4^+$ and $\text{Mo}_2\text{O}_4\text{CH}_4^+$ is not observed.

Mo_2O_5^+ and Mo_3O_8^+ ions are structurally equivalent to the MoO_2^+ ion, where one oxo ligand is changed to MoO_3 or a Mo_2O_6 group. Thus, their reactions are more likely than those of MoO_2^+ . There are some differences in product distribution. Besides, in the case of Mo_3O_8^+ formation of the $\text{Mo}_x\text{O}_y(\text{C}_2\text{H}_4)^+$ product ion is not observed. Generally, reaction mechanism for these ions is the same as for MoO_2^+ . Previously it was shown that dimers and trimers are relatively stable, so reactions should occur without Mo_xO_y^+ fragmentation.

Mo_2O_6^+ and Mo_3O_9^+ , like MoO_3^+ , are also coordinative saturated ions. Thus, they exhibit only dehydration reactions as MoO_3^+ does. The loss of oxo ligand may occur more easily due to the decrease of M^+-O bond energy with the increase of the size of oxide ion (see Table 1).

Thus, the reactions of cyclopropane dehydration occur on any single metal center surrounded by oxygen ligands, whereas only coordinative unsaturated molybdenum atoms are active in metathesis reactions. The presence of neighbor metal atoms could lead, on one hand, to decrease of molybdenum–oxygen bond energy (increases reaction rate) and to steric effects (decreases reaction rate), on the other.

Reactions with NH_3 . Reactions of different molybdenum

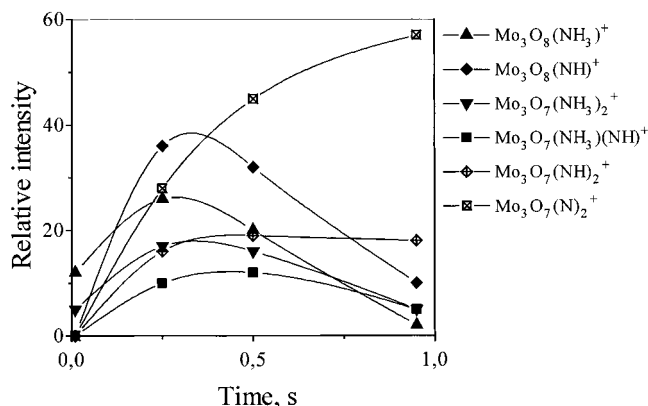
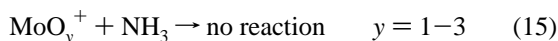


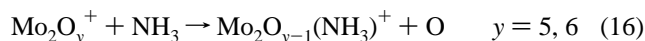
Figure 2. Kinetic curves for reaction of Mo_3O_9^+ ions with ammonia, $P(\text{NH}_3) = 1.2 \times 10^{-7}$ mbar.

oxide ions with ammonia were found to be the most interesting. In contrast to the rhenium³⁸ and osmium¹⁵ oxide ions, which twice react with NH_3 yielding the $\text{MO}(\text{NH})_2^+$ species ($M = \text{Re}, \text{Os}$), molybdenum oxide ions with one molybdenum atom do not react with ammonia at all.



The absence of dehydrogenation reactions indicates that $\text{MoO}_{y-1}-\text{NH}$ bonds are very weak (data of Table 1 give $D^\circ(\text{Mo}-\text{NH}) < 83$, $D^\circ(\text{MoO}-\text{NH}) < 105$, and $D^\circ(\text{MoO}_2-\text{NH}) < 67$ kcal/mol), whereas $\text{MoO}_{y-1}-\text{O}$ bonds are strong enough.

Molybdenum oxide ions with two molybdenum atoms are involved in the ligand-exchange reactions with ammonia molecules, reactions 16 and 17. The occurrence of these reactions was established by means of a double-resonance technique. No further conversions of ammonia molecules were found.

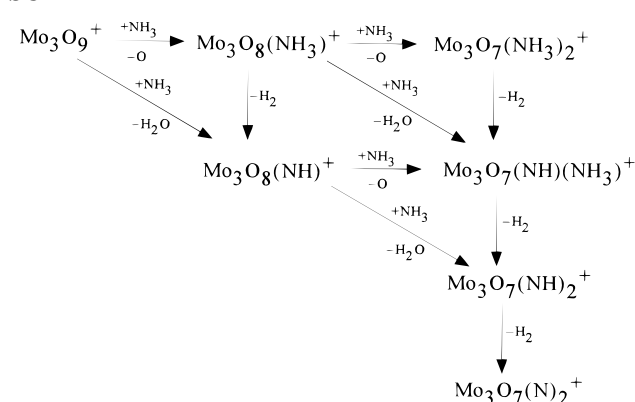


Molybdenum oxide ions with three molybdenum atoms also react with NH_3 through the exchange of their oxo ligands by ammonia. However, the consequent reactions of NH_3 dehydration were found to occur. Kinetic curves for the process of ammonia dehydrogenation by Mo_3O_9^+ ions are shown in Figure 2. $\text{Mo}_3\text{O}_8(\text{NH}_3)^+$ and $\text{Mo}_3\text{O}_8(\text{NH})^+$ products form simultaneously. This suggests that either dehydration reaction is very fast or there are two independent pathways. Other ions are the products of secondary reactions that may occur consequently. A proposed mechanism for the reaction is shown in Scheme 2.

There are two final products: $\text{Mo}_3\text{O}_7(\text{NH})_2^+$ and $\text{Mo}_3\text{O}_7(\text{N})_2^+$. Thus, two structural possibilities exist for the last one: a nitrogen molecule bound to Mo^+ or two nitrogen ligands attached to Mo^+ . However, collisions with neutral molecules (N_2) produce Mo_3O_7^+ ions but not $\text{Mo}_3\text{O}_7\text{N}^+$. These data indicate that the product ion contains one nitrogen ligand: Mo^+-N_2 .

In the case of ammonia, molybdenum oxides with different number of metal atoms have different reactivity. This may be due to weaker molybdenum-oxygen bonds in dimers and trimers that makes it possible to eliminate an O atom. Mo_3O_9^+ has a structure that differs from structures of dimers. This cluster could have an optimal Mo-Mo distance for N_2 formation. Thus, trimetallic centers of MoO_3 catalyst should be

SCHEME 2



responsible for NH_3 dehydration. Probably, these centers are also able to fix the nitrogen molecule.

Conclusion

The combination of the Knudsen cell with a standard cubic ICR trapping cell produces a number of cluster ions of molybdenum oxides Mo_xO_y^+ ($x = 1-5$, $y = 1-15$). Ionization of molybdenum trioxide vapors by electron impact yields Mo_xO_y^+ with high oxygen-to-metal ratio. Collisions with vacuum gas leads to reduction of oxygen-saturated molybdenum oxide cluster ions and to fragmentation of Mo_xO_y^+ ions with $x > 3$, whereas dimers and trimers are relatively stable.

Ion-molecule reactions of molybdenum oxide cluster ions with some small molecules have been studied. Mo_xO_y^+ ions readily oxidize a CO molecule to CO_2 . Reactions of Mo_xO_y^+ ions with cyclopropane occur through the activation of the C-C bond. The single oxo ligand has little effect on Mo^+ chemistry. Subsequent oxygens, however, completely change the reactivity. New exothermic reaction pathways occur, producing such stable ligands as CH_2 and C_2H_4 . As the number of oxygens attached to Mo^+ increases, coordinative saturation becomes more important in the reactions. This effect, undoubtedly, contributes to the differences in product ion formation seen for Mo_xO_y^+ . The increase of ion size does not affect the reactivity of molybdenum oxide cluster ions in the case of cyclopropane.

In reactions with NH_3 the reactivity of Mo_xO_y^+ ions depends on the number of metal atoms in the oxide (ion size). Molybdenum oxide monomers do not react with ammonia, whereas, dimer and trimer ions undergo the ligand-exchange reactions with ammonia and the molybdenum oxide trimers Mo_3O_8^+ and Mo_3O_9^+ dehydrogenate the NH_3 molecule yielding a complex with nitrogen.

Acknowledgment. This work was supported by the International Science Foundation under Grants RBG 000 and RBG 300.

References and Notes

- (1) Haber, J. *Chemistry and Uses of Molybdenum*, Proc. Third Int. Conf.; Climax Molybdenum Co.: Ann Arbor, MI, 1979; p 114.
- (2) Thomas, C. L. *Catalytic Processes and Proven Catalysts*; Academic Press: New York, 1970.
- (3) Delmon, B. *Chemistry and Uses of Molybdenum*, Proc. Third Int. Conf.; Climax Molybdenum Co.: Ann Arbor, MI, 1979; p 73.
- (4) Plog, C.; Weidmann, L.; Bennghoven, A. *Surf. Sci.* **1977**, *67*, 565.
- (5) Cassady, C. J.; Weil, D. A.; McElvany, S. W. *J. Chem. Phys.* **1992**, *96*, 691.
- (6) Berkowitz, J.; Inghram, M. G.; Chupka, W. A. *J. Chem. Phys.* **1957**, *26*, 842.
- (7) Kazenas, E. K.; Zvetkov, Y. V. *Zh. Neorg. Khim.* **1969**, *14*, 11.
- (8) Kazenas, E. K.; Chizikov, D. M.; Zvetkov, Y. V. In *Investigations of Processes in Metallurgy of Rare Metals*; Nauka: Moscow, 1969; p 19.

- (9) Maleknia, S.; Brodbelt, J.; Pope, K. *J. Am. Soc. Mass Spectrom.* **1991**, *2*, 212.
- (10) Michiels, E.; Gibels, R. *Anal. Chem.* **1984**, *56*, 1115.
- (11) Eller, K.; Schwarz, H. *Chem. Rev.* **1991**, *9*, 1121.
- (12) Jackson, T. C.; Jacobson, D. B.; Freiser, B. S. *J. Am. Chem. Soc.* **1984**, *106*, 1256.
- (13) Jackson, T. C.; Carlin, T. J.; Freiser, B. S. *J. Am. Chem. Soc.* **1986**, *108*, 1120.
- (14) Cassady, C. J.; McElvany, S. W. *Organometallics* **1992**, *11*, 2367.
- (15) Irikura, K. K.; Beauchamp, J. L. *J. Am. Chem. Soc.* **1989**, *111*, 75.
- (16) Elkind, J. L.; Weiss, F. D.; Alford, J. M.; Laaksonen, R. T.; Smalley, R. E. *J. Chem. Phys.* **1988**, *88*, 1622.
- (17) Irion, M. P.; Schnabel, P. *J. Phys. Chem.* **1991**, *95*, 10596.
- (18) Schnabel, P.; Irion, M. P.; Weil, K. G. *J. Phys. Chem.* **1991**, *95*, 9688.
- (19) Pan, Y. H.; Solhberg, K.; Ridge, D. P. *J. Am. Chem. Soc.* **1991**, *113*, 2406.
- (20) Irion, M. P.; Selinger, A. *Chem. Phys. Lett.* **1989**, *158*, 145.
- (21) Sharpe, P.; Cassady, C. J. *Chem. Phys. Lett.* **1992**, *191*, 111.
- (22) King, F. L.; Dunlap, B. I.; Parent, D. C. *J. Chem. Phys.* **1991**, *94*, 2578.
- (23) Parent, D. *Chem. Phys. Lett.* **1991**, *183*, 51.
- (24) Klaassen, J. J.; Jacobson, D. B. *Inorg. Chem.* **1989**, *28*, 2022.
- (25) Alleman, M.; Kellerhals, Hp.; Wanczek, K.-P. *Chem. Phys. Lett.* **1980**, *75*, 328.
- (26) Comisarow, M. V.; Parisod, G.; Grassi, V. *Chem. Phys. Lett.* **1978**, *357*, 413.
- (27) Sidorov, L. N.; Korobov, M. V.; Zhuravleva, L. V. *Mass-Spectrometrical Thermodynamic Investigations (Russian)*, Moscow University, 1985.
- (28) Chupka, W. A.; Inghram, M. G. *J. Chem. Phys.* **1953**, *21*, 371.
- (29) Kondratyev, V. N. *Chemical Bond Energies, Ionization Potentials and Electron Affinity*; Nauka: Moscow, 1974.
- (30) Martin, T. P. *J. Chem. Phys.* **1980**, *72*, 3606.
- (31) Freas, R. B.; Campana, J. E. *J. Am. Chem. Soc.* **1986**, *108*, 4659.
- (32) Freas, R. B.; Dunlap, B. I.; Waite, B. A.; Campana, J. E. *J. Chem. Phys.* **1987**, *86*, 1276.
- (33) Yu, W.; Freas, R. B. *J. Am. Chem. Soc.* **1990**, *112*, 7126.
- (34) Schiling, J. B.; Beauchamp, J. L. *Organometallics* **1988**, *7*, 194.
- (35) Kang, H.; Beauchamp, J. L. *J. Am. Chem. Soc.* **1986**, *108*, 7502.
- (36) Lias, S. G.; Bartmess, J. E.; Liebman, J. F.; Holmes, J. L.; Levin, R. D.; Mallard, W. G. *J. Phys. Chem. Ref. Data* **1988**, *17* (Suppl. 1).
- (37) Steigerwald, M. L.; Goddard, W. A. *J. Am. Chem. Soc.* **1984**, *106*, 308.
- (38) Irikura, K. K.; Beauchamp, J. L. *J. Am. Chem. Soc.* **1991**, *113*, 8344.